Experimental and LES-based Euler-Lagrange Numerical Investigation of the Particle Laden EM Induced RecerculatedTurbulent Flow Class

Mihails Ščepanskis[1],Andris Jakovičs[1],Egbert Baake[2], Bernard Nacke[2]

[1]*Laboratory of Mathematical Modelling for Environmental and Technological Processes, University of Latvia, Riga, Latvia*
[2]*Institute of Electrotechnology, Gottfried Wilhelm Leibniz University of Hanover, Hannover, Germany*

Keywords: EM, turbulent flow, particle laden flow, LES, Euler-Lagrange, modelling, experiment, ferromagnetic particles

Abstract

Experimental and numerical investigation of the particle laden recirculated turbulent flow, which is driven by EM force, is presented. Such flows are typical for induction metallurgical furnaces. The analysis is focused on the behaviour of the particles and their concentration.Experimental investigation is fulfilled utilizing the new technique: ferromagnetic particles are used as a physical model of the inclusions, such particles are separated from the samples of particle laden liquid using a permanent magnet. This experimental investigation proves the relevance of the LES-based Euler-Lagrange numerical model under dilute conditions at the quasi-stationary stage of particle distribution. As well the deposition of the inclusions on the wall of crucible was observed experimentally and investigated numerically.

Introduction

The turbulent flows of liquid metal in induction furnaces can be marked out as the certain flow class, which is characterized with several recerculation mean flow eddies in a closed volume and intensive turbulent pulsations between these eddies. Such flow can be presented in the simplest case by close turbulent melt initiated by harmonic alternating current in a cylindrical crucible with inductor around (induction crucible furnace – ICF). However, the flows of this class are observed in many other metalurgical applications: channel induction furnaces (see e.g. Baake et al. 2010), cold crucible furnaces (see e.g. Umbrashko et al. 2008), metal melting and processing technology in a levitating droplet (see e.g. Hyers 2005). The flow structure in the cross-section of the channel furnace and in the vertical central plane of ICF, cold crucible furnace and levitating droplet are qualitatively the same – several mean eddies and strong turbulent pulsations between them. These flows have the similar structure in the active region because of the same physical principle of operation.

Figure 1shows the sketch of ICF. The alternating current in the inductor creates a magnetic field and induces alternating current in the conductive liquid metal. The interaction of induced current and magnetic field results in the Lorentz force, which drives the liquid away from the wall and forms the two-eddy structure. However, the power of IMFs is sufficiently high to produce a turbulent flow with a high Reynolds number (e.g. for laboratory ICF it is about 1e+5). Therefore the two mentioned vortices appear only in the time averaged case but in practice at each moment the turbulent flow consists of numerous eddies with different sizes, however, the common structure of the flow remains quasi-stationary (statistically stationary).

The distribution of mean velocity of liquid metal flowcreated by single-phase alternating magnetic field have been studied experimentally in many published papers even in the 80s (see e.g.Trakas et al. 1984).The numerical two-equation models for the effective turbulent viscosity (quasi-steady flows) led to the satisfactory results for time averaged quantities (see e.g. El-Kaddah&Szekely 1983, Baake et al. 1995, Bojarevics et al. 1999). Later Umbrashko et al. (2006) and Kirpo et al. (2007)carried out the experiment withthe permanent magnet probe and observed the long period fluctuations between the mean eddies.These authors also showed that the LES should be used to obtain the observed pulsations numerically, that became possible only in the last decade. The effective heat and mass transport between mean eddies are fulfilled mostly by this pulsation, hence, LES should be utilized for such flow class.

Obviously, this flow class significantly differs from the well-studied turbulence in a pipe, a channel and other classical flows. It also differs from the turbulent flow in the gap between two counterrotating disks (the von Kármán flow) due to the intensive axial pulsations between the main eddies near the wall, which has already been discussed. Therefore, the investigation of this flow class is interesting also from the fundamental point of view. As it was already mentioned, the single-phase flow case is enough researched (see the previous paragraph). However, the two-phase case and, particularly, particle laden flow is still poor investigated. Solid particles are wide spread in the liquid metal flows in metallurgical equipment: artificial alloying additions, oxides from dirty secondary metals, products of the wall erosion. Thus, the study of the particle laden EM induced recirculated turbulent flow class is essential from the both fundamental and practical point of view.

The EM field directly influences the non-conducting particles in the conducting liquid within the penetration depth and transport them to the wall (Lennov&Kolin 1954),

which is another specific aspect of the considered system. The layer of significant EM field is sufficiently thin (about 20% of the radius of the crucible – δ/R = 0.2). Due to the non-slip boundary conditions the flow velocity is zero at the wall and it increases in a radial direction until it rapidly achieves the maximal value at the relative distance Δ/R = 0.04 from the wall (see Figure 2). $\delta>\Delta$, therefore, the maximum velocity is inside the layer of EM penetration. Obviously, particles move preferentially in the streamline of maximal velocity. Therefore, the major part of the particles comes frequently to the layer of significant EM field. The particle motion in turbulent flows without EM is well researched (see e.g. Toschi&Bodenschatz 2009), but it is not possible to separate the large interior zone without EM field from a thin layer near the wall and one should consider the motion of the particles in the whole volume.

Previously, McKee et al. (1999) proposed the significantly simplified analytical model for the calculation of the non-conductive particle path in rotating magnetohydrodynamic flow within a long cylinder. Later, Kirpo et al. (2009) used FLUENT software to investigate the behaviour of a particle cloud in the turbulent flows inside the induction furnaces. This model was sufficiently rough: only drag, buoyancy and EM forces were taken into account for the calculations of the particle motion. The model used by Kirpo was enhanced through the development of OpenFOAM software code: the Lagrange equation was supplemented with lift, acceleration and added mass forces. The significance of these forces was statistically proved by Ščepanskisetal. (2011).

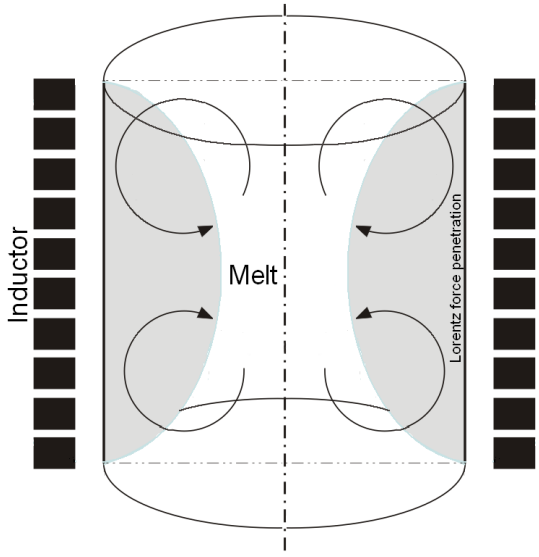

Figure 1: The sketch of ICF.

Despite the relative success in the Lagrange modeling of such particle laden flow, lack of the experimental investigations till now was the significant problem in order to verify the numerical models. The electric well-conductive materials are not optically transparent but transparent liquids have low conductivity. Sadoway&Szekely (1980) tried to use transparent LiCl-KCl eutectic to reproduce the recirculation motion in an ICF, however, they failed to do this. EM field does not only produce the induced flow motion, but also heat up the liquid within the penetration depth. Thereby, the thermal convection dominates in the low-conductive transparent liquids. In spite of the optimistic conclusions of Sadoway&Szekely (1980), the simulation, which is done by the authors of the present paper, shows that it is not possible to avoid the thermal motion by changing the EM conditions. Therefore this liquid cannot be used to produce such flow patterns. The only one more or less successful method, developed by Taniguchi &Brimacombe (1994), provides an opportunity to investigate experimentally the rate of the particle deposition in a flow of liquid metal under EM force. However, because the results are obtained by cutting solidified liquid, it is impossible to receive any information about the dynamics of the process inside the melt using such experimental technique. Moreover, the presence of the solidification front has influence on the particles during the solidification and it is not clear, if this effect is negligible.

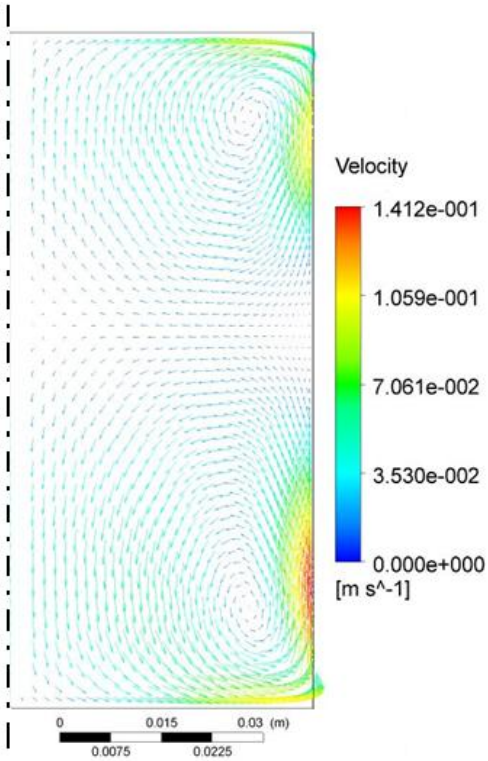

Figure 2: The average flow in half of symmetry plane of ICF (calculated using k-ε turbulence model).

Finally, the present paper proposes the original experimental technique, which uses ferromagnetic particles. This experiment is allowed to verify the numerical model. The technique and the results are described in details below.

Nomenclature

u	velocity ($m \cdot s^{-1}$)
g	free fall acceleration ($m \cdot s^{-2}$)
j	current density ($N \cdot m^{-3}$)
B	magnetic flux (T)
f	force density ($N \cdot m^{-3}$)
e	unity vector
t	time (s)
d	diameter of the particle (m)

Greek letters

ρ	density ($kg \cdot m^{-3}$)
ν	kinematic viscosity ($m^2 s^{-1}$)

σ electric conductivity ($S \cdot m^{-1}$)
μ magnetic permeability ($N \cdot A^{-2}$)
μ_0 magnetic permeability of free space ($N \cdot A^{-2}$)
γ rate of semi-soft collision of particles with the wall

Subsripts
p particle
f flow of the liquid
0 amplitude of the harmonic functions
r radial component of a vector
φ angular component of a vector
z axial component of a vector
⊥ normal to the wall component of a vector
‖ parallel to the wall component of a vector

Numerical Model

The present model includes the simulation of the flow and the particle motion. The flow is driven by EM force and thermal buoyancy force in the Boussinesq approximation. The turbulence is calculated using LES method with the isotropic Smagorinskysubgrid viscosity model. The solid inclusions are calculated adopting the LES-based Euler-Lagrange approach in the limit of dilute conditions (one-way coupling). This assumption is possible because the volume of the inclusions does not exceed 0.1% of the liquid volume. The rigid spheres are also assumed. The following Lagrange equation describes the motion of the inertialelectrically non-conductive (oxide)spherical particles (Ščepanskis et al. 2011):

$$\underbrace{\left(1+\frac{C_A}{2}\frac{\rho_f}{\rho_p}\right)\frac{\mathrm{d}\boldsymbol{u}_p}{\mathrm{d}t}}_{\frac{\mathrm{d}u_p}{\mathrm{d}t}+\text{added mass force}} = \underbrace{C_D\boldsymbol{U}}_{\text{drag force}} + \underbrace{\left(1-\frac{\rho_f}{\rho_p}\right)\boldsymbol{g}}_{\text{buoyancy force}} - \underbrace{\frac{3}{4}\frac{1}{\rho_p}Re(\boldsymbol{j}_0\times\boldsymbol{B}_0^*)}_{\text{EM force}} + \underbrace{\frac{\rho_f}{\rho_p}C_L\cdot[\boldsymbol{U}\times\mathrm{rot}\boldsymbol{U}]}_{\text{lift force}} + \underbrace{\left(1+\frac{C_A}{2}\frac{\rho_f}{\rho_p}\right)\frac{\mathrm{D}\boldsymbol{u}_f}{\mathrm{D}t}}_{\text{acceleration + added mass}}, \quad (1)$$

where $\boldsymbol{U}=\boldsymbol{u}_f-\boldsymbol{u}_p$, D/D$t$ means material derivation, $C_A=2.1$ is acceleration coefficient, which is expressed for $Ac=U^2d^{-1}\cdot(dU/dt)^{-1}\gg 1$ (Odar & Hamilton 1964); $C_D(U)$ and $C_L(U)$ are non-linear drag and lift coefficients in Schiller & Naumann (1933) and Legendre & Magnaudet (1998) approximations respectively. The approximations for the coefficients are chosen analyzing statistically non-dimensional parameters $Re_p=d\cdot U/\nu$, $Sr=\left|\partial\boldsymbol{u}_f/\partial\boldsymbol{s}\right|\cdot d/U$, $\boldsymbol{s}$ is unit vector perpendicular to $\boldsymbol{U}$ (Ščepanskis et al. 2011).

Concerning collisions of the particle with the wall, the semi-soft model is applied: $\boldsymbol{u}''_{p,\perp}=-\gamma\cdot\boldsymbol{u}'_{p,\perp}$, $\boldsymbol{u}''_{p,\parallel}=\gamma\cdot\boldsymbol{u}'_{p,\parallel}$ where double prime means the velocity after collision, but single prime means the velocity before the collision with the wall.$\gamma=0.8$unless otherwise defined.

The mentioned numerical algorithm is coded using the open source OpenFOAM libraries and solvers.

Experimental Technique

A small glass-wall crucible is used for the experimental investigation. Size and the EM parameters of ICF are shown on Table 1. The low temperature Wood's alloy (50% Bi – 26.7% Pb – 13.3% Sn – 10% Cd eutectic), which becomes liquid at 70°C, was used as the model liquid metal. Such equipment induces 1.3 kW power in the melt that leads to heating with rate 1.8 °C·s^{-1}. Thus, the maximal duration of the experiment is limited, until the melt achieves 150 °C, which is the critical temperature for evaporation of the toxic cadmium from the alloy.

Table 1: Size and EM parameters of the experimental ICF.

Radius	4.5 cm
Height (melt & inductor)	10 cm
Frequency	4 kHz
Current	432 A
No. of turns	6

10.5 g of the spherical iron particles with diameter 250-350 μm are placed on the open surface of the liquid metal, which generally corresponds to the industrial case of the admixing of alloying particles in ICF. The power of the furnace is switched on when the particles are already on the surface, it is done in the attempt to reduce the operation time of the furnace and thereby avoid the Wood's metal from dangerous overheating. Obviously, this case differs from the industrial conditions, where the inclusions are usually placed on the surface of the already stirring metal. However, the measurements of the particle concentration are carried out at 11th s, when the transition regime is already passed. The local 4 ml probes of the particle laden Wood's metal are taken. Table 2 contains the comparison of the conditions in the experiment and the simulation. The iron particles are collected from the liquid sample using a strong permanent magnet and counted after that.

Table 2: Comparison of the conditions in the experiment and the simulation.

	experiment	simulation
number (mass) of the particles	10.5±0.1 g (≈9e+4 particles)	83 635 particles
size of the particles	250 – 350 μm	300 μm
material (density) of the particles	iron (Fe) – well conductive, ferromagnetic	7 874 kg·m^3, non-conductive, non-magnetic
volume of sample (experiment) and the zone of numerical analysis	4±1 ml	Toroidal zone with approximately 36 mesh cells in the cross section
correspondence of the experimental and simulated results	number of particles in the sample	(number of particles in the proper region) × (vol. of the sample) / (volume of the numerical zone)

The present technique proposes to use iron particles as a physical model for the tracking of non-conductive (oxide)

inclusions in ICF. The described experimental technique is very useful because the ferromagnetic particles can be easily separated from the liquid metal with the permanent magnet. The described experimental investigation of the distribution of solid particles in the flow of liquid metal is the only successful experiment, known by the authors.

Before discussion of the results, the influence of EM force on oxide and iron particles should be additionally described. Generally, the time dependent EM force should be written as follows (the average expression of the force is placed in the equation (1)):

$$\boldsymbol{f}_{EM} = -\frac{3}{2}\frac{\sigma_f-\sigma_p}{2\sigma_f+\sigma_p}(\boldsymbol{j}\times\boldsymbol{B}) + \frac{\mu-\mu_0}{4\mu\mu_0}\nabla B^2, \qquad (2)$$

where **j** and **B** are harmonic time dependent vectors. The poor conductive ($\sigma_p << \sigma_f$) inclusions are usually used in the metallurgical applications, and they are non-magnetic ($\mu = \mu_0$). Thereby, the equation (2) is reduced to the following expression:

$$\boldsymbol{f}_{EM,oxide} = -\frac{3}{4}(\boldsymbol{j}\times\boldsymbol{B}) = -\frac{3}{4\mu_0}\left((\boldsymbol{B}\cdot\nabla)\boldsymbol{B} - \frac{1}{2}\nabla B^2\right). \qquad (3)$$

In the area of the maximal magnetic flux – at the middle of the inductor – B_r and B_φ are negligible. Therefore, the first term in equation (3) can be reduced to $3/(4\mu_0)\cdot \boldsymbol{e}_z \cdot B_z \cdot \partial B_z/\partial z$ that is also negligible because $\partial B_z/\partial z \approx 0$. Thus, the term $(\boldsymbol{B}\cdot\nabla)\boldsymbol{B}$ is much less than the second term in (3) at the middle of the inductor:

$$\boldsymbol{f}_{EM,oxide} \approx \frac{3}{8\mu_0}\cdot\nabla B^2. \qquad (4)$$

On the contrary, iron is a good conductor ($\sigma_p > \sigma_f$) and a ferromagnetic material ($\mu >> \mu_0$) but due to the partial wetting and the transitional resistance, we can assume the equal conductivity of the particle and the liquid. Therefore, for this type of particles equation (2) can be reduced to

$$\boldsymbol{f}_{EM,iron} = \frac{1}{2\mu_0}\cdot\nabla B^2. \qquad (5)$$

Apparently, the equations (4) and (5) shows that $f_{EM,oxide} \approx f_{EM,iron}$ at the middle of inductor. The results of the EM simulation on Figure 3 also confirm the coincidence of the forces in the middle zone of the crucible, however, $f_{EM,iron} \approx 3/2 \cdot f_{EM,oxide}$ in the zone of the flow vortices. Despite the noncritical differences between the forces $f_{EM,iron}$ and $f_{EM,oxide}$ in the upper and lower eddies, it is possible to conclude that iron particles can be used as the rough physical model of the typical metallurgical inclusions in the induction furnaces.

Results and Discussion

Three different aspects of the particle behaviour in the liquid metal flow of ICF are discussed in the present paper: 1) the initial stage of the particle admixing from the surface of the melt; 2) quasi-stationary distribution of the solid inclusions in the melt; 3) deposition of the non-conductive inclusions on the wall. All mentioned types of the particle behaviour take place in the flow of ICF and together describe the common behaviour of inclusions in such flow, that is, in the industrial case of admixing inclusions in induction furnaces.

Many alloys are formed by admixing solid inclusions in the liquid melt (e.g. carbon in steel). According to the widespread induction technology, the inclusions are placed on the open surface of the liquid metal in the same ICF, where it has been melted previously. Figure 4 a shows the initial placing if inclusions on the surface of the liquid metal. Then, the intensive turbulent flow of alloy mixes the solid particles into the melt in spite of their low density (usually the density of non-metallic inclusions is lower than the density of liquid metal).

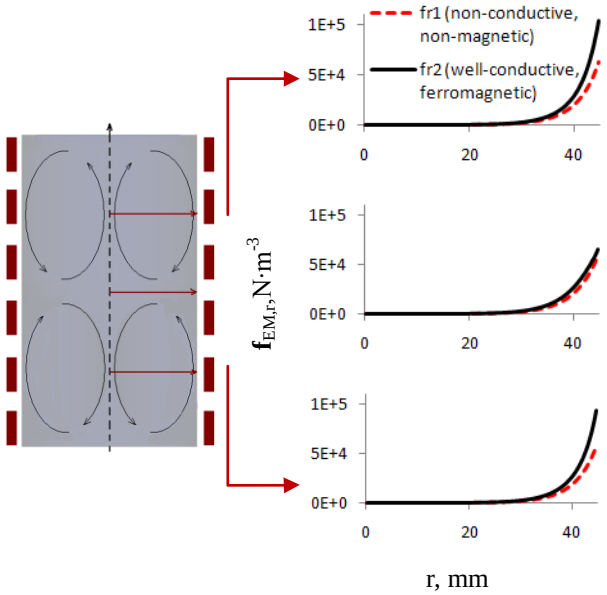

Figure 3: Magnitude of the EM force density (radial component) in the case of non-conductive & non-magnetic and well-conductive & ferromagnetic particles (see equations (3) and (5) respectively).

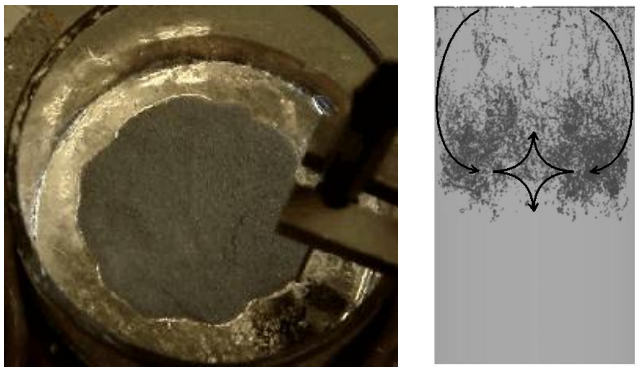

(a) (b)

Figure 4: (a) Solid inclusions on the top surface of the melt in the laboratory ICF – initial position; (b) the scheme of motion of the inclusions from the initial position on the surface (vertical cross section of the crucible, simulated result).

The scheme of initial motion of particle cloud is shown on Figure 4 b. Initially, the cloud follows the flow motion and moves to the surface-wall corner. It is observed that the significant surface tension and partial wettability of the particles leads to difficulties to get the inclusions inside the melt. Industrial and experimental observations testify that the power of the ICF (i.e. intensity of the flow) should be increased to get the initial cloud inside the liquid. The furnace can be operated with lower power after that.

When the particles get in the melt at the surface-wall corner, they follow the flow and move down to the middle zone of the crucible, where the flow change the direction and moves to the axis of symmetry the crucible (see Figure 1 and Figure 2). As it was already discussed, EM force act on the particle in the direction to the wall, when it is within the

penetration depth. Therefore, the initial cloud of the inclusions is affected by EM field and moves down close to the wall. Some particles even deposit on the wall, this phenomenon will be discussed later.

Then, the initial cloud is significantly decelerated in the middle of the crucible by flow, which changes the direction. The decelerated cloud is blurred and separates to the one, which moves in the upper part of the crucible, and the second part of particles goes to the lower part of ICF. Strong oscillations of the flow at the middle of crucible are observed (Umbrashko et al. 2006, Kirpo et al. 2007). Ščepanskis et al. (2012) found the similar oscillation of the particles between the upper and lower eddies. Finally, such oscillating exchange of the particles between mentioned zones leads to the axial homogenization of the inclusions in the melt.

Figure 5 demonstrates the dynamics of concentration of the particles in the ICF at the different height (simulated results). At the first stage (0 – 4 s) significant peaks appear in the upper and middle zone of the crucible (2nd and 5th zones respectively). This corresponds to the initial motion of the cloud in the mean upper eddy. After that the particles comes to the lower eddy too, the initial cloud is blurred and the concentration increases in the middle of eddies (4 – 10 s). Figure 5 shows that the quasi-stationary stage in the particular ICF starts at 10th s. The exchange of the inclusions between zones achieves the dynamic equilibrium at this stage.

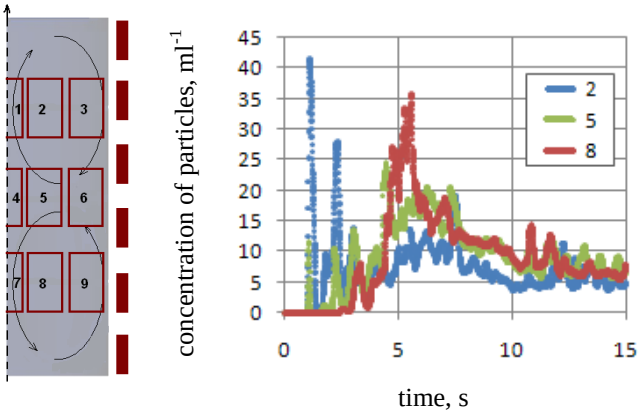

Figure 5: Dynamics of concentration of the particles in the different areas (simulated results). Areas are numbered on the sketch of the crucible (left image).

The concentrations of the inclusions at the quasi-stationary stage are shown on Figure 6. The experimental results at this stage were also obtained, using the new experimental technique, which was described above. The experimental results are in the good agreement with the numerical LES-based Euler-Lagrange results. Thus, this experimental investigation proves the relevance of the used numerical model (see equation (1) and the proper paragraph).

Nevertheless, the small differences of the experimental and numerical results at 3rd – 6th points can be observed on Figure 6. These differences as well as the general distribution will be discussed in details now. As it was already mentioned, the cloud of the particles following the main eddies frequently comes to the near wall region with the strong EM field. As far as the force directly acts the particle and moves it to the wall, the concentration of the inclusions near the wall (right points on the curves) is higher than in the bulk of the melt. This trend is more appreciable in the middle zone of the crucible. EM force is stronger there and the average flow is slower, that means that other inertial forces (see equation (1)) are less compatible than EM force. Now let us analyze the difference between the experimental and numerical results. It was observed during the experiment, that the iron spheres magnetize and make small clusters. Hence, the effective size of the inclusions increases within the penetration depth of EM field. It was already obtained previously (Ščepanskis et al. 2010) that the relative balance between forces changes and EM force have greater influence with increase of the size of inclusions. However, the present numerical model does not take into account the effect of magnetization and clustering of the inclusions. Therefore the small difference between numerical and experimental results appears at the 3rd point. However, this difference is only the effect of second order. The same difference remains at the whole curve of middle zone (4th – 6th points). Following the general scheme of the particle motion (Figure 4 b), the inclusions come to this zone through the area of the 3rd point. Therefore, apparently, the difference, which appears due to the clustering of ferromagnetic particles at the 3rd point, leads to the same difference in the middle zone (4th – 6th points). But the oscillating exchange between the upper and lower zones (see Ščepanskis et al. 2012)minimizes this effect at the lower curve (7th – 9th points).

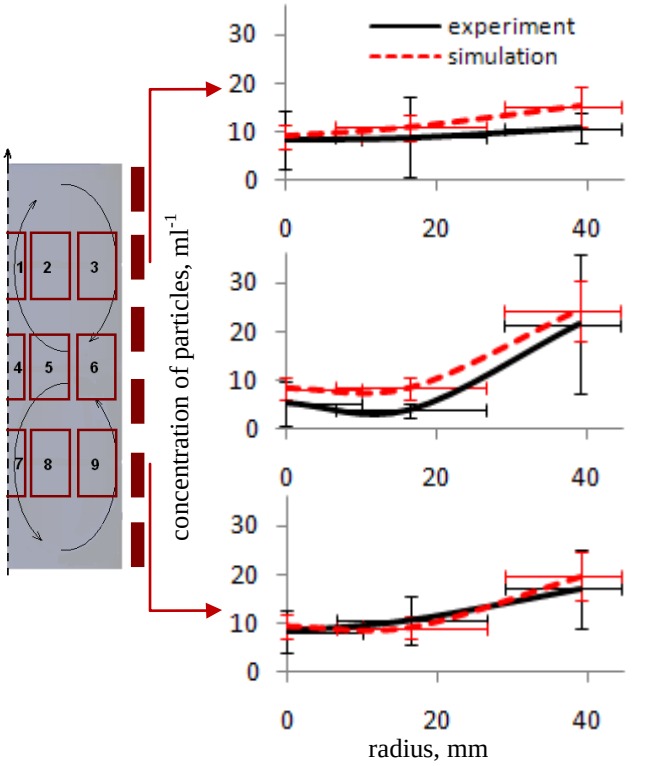

Figure 6: Experimental and numerical results of the concentration of solid 300±50 μm inclusions in the flow of ICF at 11±2 s from the beginning of stirring (quasi-stationary regime). Experimental samples were taken in the areas, they are marked with the red rectangles on the sketch of the crucible (left image).

The mentioned EM influence effect on the particles, which is even increased by clustering of iron particles, leads to the deposition formation on the wall. Such formation was

observed in the experimental crucible, when it was drained after the experiment (Figure 7). The numerical results on Figure 8, which show the dynamics of axial distribution of surface concentration of deposited particles in ICF, also confirm the concentration of deposited particles in the upper part of the crucible. In both numerical and experimental cases the density of inclusions' material was less than the liquid density. Therefore, this result is expected.

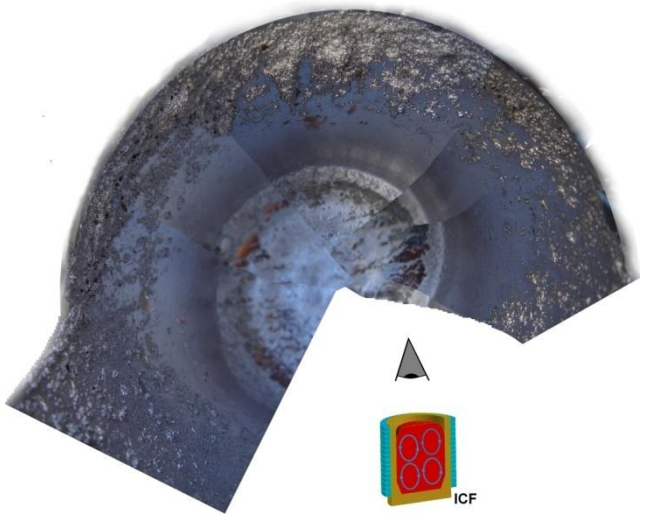

Figure 7: Deposition formation of iron particles on the walls of the experimental crucible. The ICF was drained after the experiment. This image is made from several photos of the crucible, viewing it from the top to the bottom.

The process of deposition also continues during the whole period of simulation. The lines on the plots on Figure 8 mean that the particles are delivered to the wall in discrete portions. The time between these portions is approximately equal to the turnover of the mean vortex. Figure 8 also shows that the deposited particles slip down by the wall in the direction of positive EM field gradient.

Different plots on Figure 8 stand for the simulations with the different rate of semi-soft collision of particles with the wall γ. There is no significant difference between the plots on Figure 8. Therefore, we can conclude that different types of the collisions with the wall can lead only to the effects of the second order. The strong EM force defines the dominating behavior of the inclusions close to the wall of the crucible.

Conclusions

The new experimental approach for investigation of the quasi-stationary distribution of solid inclusions in the flows of liquid metal is proposed. The iron particles areused as a physical model for the tracking of non-conductive inclusions in ICF. The described experimental technique is very useful, because the ferromagnetic particles can be easily separated from the liquid metal with the permanent magnet. Thus, the experimental verification of the numerical model for particle distribution in non-transparent liquid metal was fulfilled for the first time. The experiment showed satisfactory agreement with the numerical results, which were obtained using the LES-based Euler-Lagrange model under dilute conditions.

Numerical analysis of the particle behavior in the turbulent flow of liquid metal in ICF allowed to mark out 3 stages of behavior of the initial cloud, which was situated on the top surface of the melt (as in the industrial case of admixing inclusions in ICF).

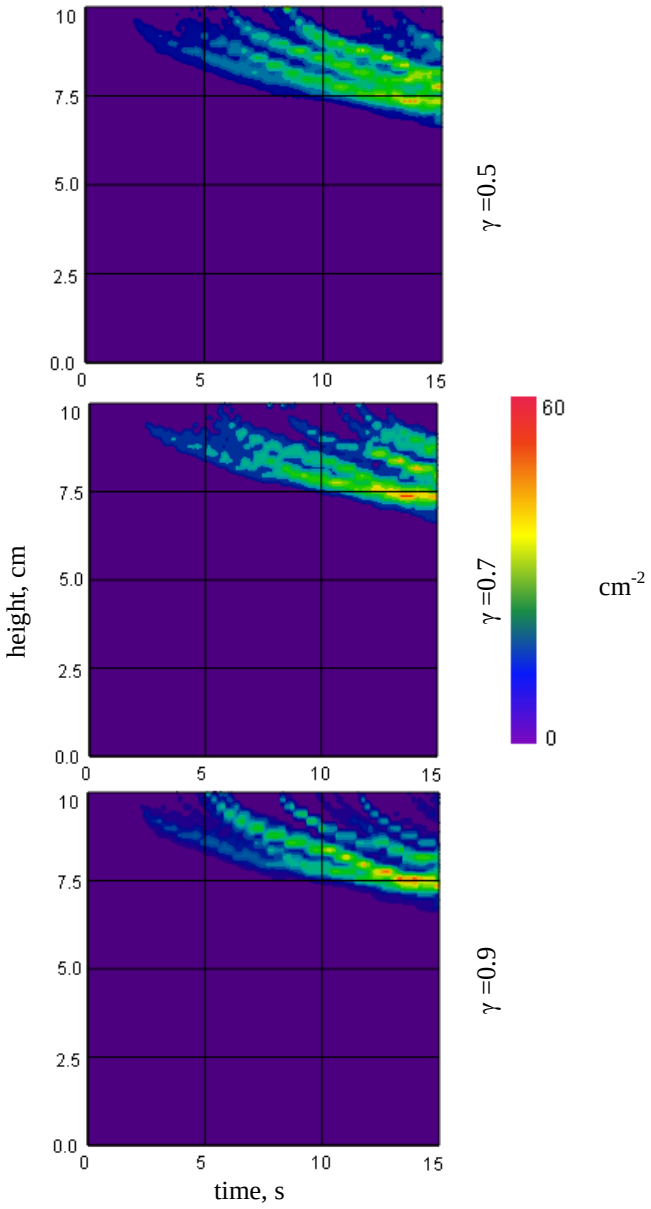

Figure 8: Time dependence of axial distribution of surface concentration (cm^{-2}) of the deposited 300 μm particles in ICF. Liquid-to-particle density rate is equal to 1.5. Parameter γis the rate of semi-soft collision with the wall.

Initially, the cloud moves to the surface-melt corner, where the surface tension and wettability effect significantly influence admixing of the cloud. After that, the cloud goes down to the middle zone of the melt, where it separates to the one, which remains the motion in the upper eddy, and the second sub cloud, which goes to the lower part of the crucible.

The sub clouds are blurred during the second stage of the mixing. The concentration of solid inclusions increases in the centres of the mean eddies. Also the oscillating exchange of the particles between the upper and the lower eddies begins.

The third quasi-stationary stage of the particle distribution is fulfilled by dynamic equilibrium in the exchange between the different zones of the crucible. The experimental and numerical results show at this stage the increase of the

concentration near the wall of ICF due to the direct influence of EM field on the inclusions.
Finally, the numerical investigation of the particle behaviour near the wall of the crucible finds the deposition process on the wall. The reason of the deposition formation is also strong influence of EM force. This process starts at the first stage of mixing and continues the whole time of the operation of ICF. However, the particles are delivered to the wall in the discrete portions, which correlates with the turnover of the mean eddy. The deposited particles slip in the direction of positive force gradient. The numerical results also show that the particle friction with the wall and the rate of semi-soft collision with the wall influence the deposition process insignificantly.

Acknowledgements

The contribution of M. Ščepanskis is sponsored by the European Social Fund within the project "Support for Doctoral Studies at University of Latvia". The authors also thank the organizers of ICMF conference for financial support for student, which allows to cover the huge expenses of the trip.
The authors also thank M. Geža and P. Turewicz for support during planning and carrying out the experiment.

References

Baake, E., Muhlbauer, A., Jakowitsch, A., Andree, W. Extension of the k-ε model for the numerical simulation of the melt flow in induction crucible furnaces. Met. Mater. Trans. B, Vol. 26B, 529-536 (1995)

Baake, E., Jakovičs, A., Pavlovs, S., Kirpo, M. Long-term computations of turbulent flow and temperature field in the induction channel furnace with various channel design. Magnetohydrodynamics,Vol. 46, 461-474 (2010)

Bojarevics, A., Bojarevics, V., Gelfgat, Yu., Pericleous, K. Liquid metal turbulent flow dynamics in a cylindrical container with free surface: experiment and numerical analysis. Magnetohydrodynamics,Vol. 35, No. 3, 205-222 (1999)

El-Kaddah, N.& Szekely, J. The turbulent recirculating flow field in a coreless induction furnace, a comparison of theoretical predictions with measurements. J. Fluid. Mech.,Vol. 133, 37-46 (1983)

Hyers, R. W. Fluid flow effects in levitated droplets. Meas. Sci. Technol,Vol. 16, 394-401 (2005)

Kirpo, M., Jakovičs, A., Baake, E., Nacke, B. Analysis of experimental and simulation data for the liquid metal flow in a cylindrical vessel. Magnetohydrodynamics,Vol. 43, No. 2, 161-172 (2007)

Kirpo, M., Jakovičs, A., Baake, E., Nacke, B. LES study of particle transport in turbulent recirculated liquid metal flows. Magnetohydrodynamics, Vol. 45, 439-450 (2009)

Legendre, D.& Magnaudet, J. The lift force on a spherical bubble in a viscous linear shear flow. J. Fluid Mech.**,Vol.** 368, 81-126 (1998)

Lennov, D.& Kolin, A. Theory of electromagnetophoresis. I. Magnetohydrodynamic forces experienced by spherical and symmetrically oriented cylindrical particles. J. Chem. Phys.,Vol. 22, 683-689 (1954)

McKee, S., Watson, R., Cuminato, J. R., Moor, P. Particle-tracking within turbulent cylindrical electromagnetically-driven flow. Int. J. Numer. Meth. Fluids, Vol. 29, 59-74 (1999).

Odar, F.& Hamilton, W. S. Forces on a sphere accelerating in a viscous fluid. J. Fluid Mech.,Vol. 18, 302-14 (1964)

Sadoway, D. R.& Szekely, J. A new experimental technique for the study of turbulent electromagnetically driven flows. Metall. Trans. B, Vol. 11B, 334-336 (1980)

Ščepanskis, M., Jakovičs, A., Baake, E. Statistical analysis of the influence of forces on particles in EM driven recirculated turbulent flows. J.Phys.:Conf.Ser., Vol. 333,012015(2011)

Ščepanskis, M., Jakovičs, A., Baake, E.,Nacke, B. Analysis of the oscillating behavior of solid inclusions in induction crucible furnaces.Magnetohydrodynamics, Vol.48, No.4, 677-686 (2012)

Schiller, L.& Naumann, Z. Uber die grundlegenden Berechnungen bei der Schwerkrafttaufbereitung (in German). Ver. Deut. Ing.,Vol. 77, 318-20 (1933)

Taniguchi, S.& Brimacombe, J. K. Application of pinch force to the separation of inclusion particles from liquid steel. ISIJ International, Vol. 34, 722-731 (1994)

Toschi, F.& Bodenschatz, E. Lagrangian properties of particles in turbulence. Annu. Rev. Fluid. Mech.,Vol. 41, 375-404 (2009)

Trakas, C., Tabeling, P., Chabrerie, J. P.Etude experimentale du brassage turbulent dans le four a induction (in French). J. Méc. Théor. Appl., Vol. 3, 345-370 (1984)

Umbrashko, A., Baake, E., Nacke, B., Jakovics, A. Modeling of the turbulent flow in induction furnaces. Met. Mater. Trans. B,Vol. 37B, 831-838 (2006)

Umbrashko, A., Baake, E., Nacke, B., Jakovics, A. Thermal and hydrodynamic analysis of the melting process in the cold crucible using 3d modelling. Heat Transf. Res.,Vol. 39, 413-421 (2008)